JSAE 20159212
SAE 2015-YY-YYYY

Impact of Effective Compression Ratio on Gasoline-Diesel Dual-Fuel Combustion in a Heavy-Duty Engine Using Variable Valve Actuation

Andrew Ickes, Reed Hanson, Thomas Wallner
Argonne National Laboratory

ABSTRACT

Dual-fuel combustion using port-injected gasoline with a direct diesel injection has been shown to achieve low-temperature combustion with moderate peak pressure rise rates, low engine-out soot and NO_x emissions, and high indicated thermal efficiency. A key requirement for extending high-load operation is moderating the reactivity of the premixed charge prior to the diesel injection. Reducing compression ratio, in conjunction with a higher expansion ratio using alternative valve timings, decreases compressed charge reactivity while maintain a high expansion ratio for maximum work extraction.

Experimental testing was conducted on a 13L multi-cylinder heavy-duty diesel engine modified to operate dual-fuel combustion with port gasoline injection to supplement the direct diesel injection. The engine employs intake variable valve actuation (VVA) for early (EIVC) or late (LIVC) intake valve closing to yield reduced effective compression ratio. Testing was conducted at a mid-load operating condition using a gasoline-diesel dual-fuel operating strategy. The impact on dual-fuel engine performance and emissions with respect to varying effective compression ratio is quantified within this study.

As effective compression ratio is reduced, overall massflow through the engine decreases, yielding both higher gas exchange efficiencies and increased heat transfer losses. With constant combustion phasing gasoline/diesel fueling fraction, and NO_x emissions held constant, overall brake thermal efficiency remains relatively constant across effective compression ratios.

INTRODUCTION

Strict new standards for CO_2 emissions and fuel consumption of heavy-duty engines and vehicles [1], coupled with the business interests of heavy-duty vehicle operators to reduce total cost of operation, drive an increased push for high-efficiency heavy-duty motive power. Stringent emissions standards also mandate low system-out (including engine and aftertreatment) levels of gaseous (including NO_x and NMHC) and particulate emissions [2]. Reflecting the need for higher efficiency heavy-duty engines, key objectives of the Department of Energy (DOE) SuperTruck program include the demonstration of a heavy-duty engine with 50% brake thermal efficiency and establishment of a pathway to 55% brake thermal efficiency [3]. Many previously developed low-temperature diesel combustion strategies produce low engine-out emissions but frequently at the penalty of lower engine efficiency. However, increasingly effective aftertreatment systems for heavy-duty diesel engines have enabled higher overall engine efficiency [4] – combustion concepts designed to produce low engine-out emissions must therefore also deliver comparable efficiencies to remain competitive. Dual-Fuel combustion concepts were developed as a method of addressing the limitations of earlier low-temperature combustion strategies while providing high engine efficiency.

By introducing two fuels of differing reactivity into the combustion chamber separately, overall fuel reactivity levels can be adjusted with operating conditions. Further, separating the fuel delivery, port-injecting the low reactivity fuel and direct injecting the high reactivity fuel, has been shown to create in-cylinder reactivity stratification, slowing combustion and decreasing the pressure rise rate, a primary load-limiting factor for many HCCI-type combustion strategies [5,6]. Dual-fuel strategies using gasoline and diesel have shown potential for high efficiency, both quantified by indicated thermal efficiency measurements on single-cylinder engines [5,6] and by brake thermal efficiency measurements on multi-cylinder engines [7,8,9]. By using a low compression ratio, it has been shown that a dual-fuel concept can cover the entire operating range of a heavy-duty engine [10]; efficiency with the low compression ratio, however, may not offer advantages over current single-fuel conventional diesel engines.

Different variations on the dual-fuel concept have been explored, with key differences being the delivery conditions of the diesel injection. The Reactivity Controlled Compression Ignition (RCCI) concept uses

very early injection timing with relatively low injection pressure – start of combustion and subsequent combustion phasing is largely kinetically driven [5,6]. A similar concept, denoted as 'CM2' has also been reported in literature [8,11,12]. However, by using a more conventionally timed, high pressure, single diesel injection, greater control over the combustion phasing can be achieved and, depending on the thermal boundary conditions, potentially an expansion of the upper load limit of the operating range can be accomplished [7,8,9].

Early development studies on RCCI operation were conducted on an engine which used a camshaft profile yielding late closing of the intake valve, at 85°BTDC, which reduced the geometric effective compression ratio of the engine to 9.1:1 [5,13,14]. This late IVC timing and lower effective compression ratio was utilized to reduce peak compression pressure and temperature, reducing overall charge reactivity for control over resultant combustion phasing. The same group reverted to more conventional IVC timing (IVC timing of 143°BTDC, geometric effective CR of 15.1:1) for their test engine in later publications on RCCI development [6,15,16].

Manipulation of the intake valve timing, the genesis being the concept proposed by Miller [17], is effective for controlling trapped in-cylinder charge mass and, subsequently, the peak compression pressure and temperature. By closing the intake valve earlier than conventional (during the intake stroke), referred to as early intake valve close (EIVC), the valves are closed before full aspiration of the maximum swept cylinder volume occurs. The continued downward motion of the piston expands the trapped charge to below ambient conditions before the start of compression. By closing the intake valves after conventional timing during the compression stroke, late intake valve close (LIVC), the full cylinder volume is drawn during the intake stroke, but a portion of the cylinder charge is expelled through the still (partially) open intake valves during the start of the compression stroke. Both EIVC and LIVC methods result in reduced effective compression, decreasing the effective compression ratio and lowering peak compression pressure and temperature.

The use of both early [18,19,20,21] and late [22] timing of the intake valve closing have been explored for conventional, diffusion-controlled, diesel combustion. These valve strategies were investigated primarily to reduce NO_x emissions through the reduction of peak compression pressure and temperature, due to the lower effective compression ratio and, as a result, decrease the resulting peak combustion temperatures. These reductions in NO_x emissions were frequently accompanied by a corresponding increase in soot emissions. Additionally, in some cases, an improvement in brake specific fuel consumption (BSFC) was observed [19,22].

The impact of EIVC [23] and LIVC [22,24,25,26] valve strategies on premixed low-temperature combustion strategies (LTC, PCI, PCCI) have also been covered in the literature. As with conventional diesel combustion, one primary objective is to reduce NO_x emissions by reducing peak combustion temperatures by way of decreasing the effective compression ratio and resulting conditions at the end of compression. In addition, the lower effective compression ratio helps extend the ignition delay, improving mixing of the diesel injection prior to the onset of combustion and, unlike for diffusion controlled conventional diesel combustion, reducing soot emissions. These same results were also achieved in a range of studies on premixed low-temperature diesel combustion by reducing base geometric compression ratio. With many diesel LTC strategies limited to lower engine load conditions, the use of variable camshaft timing was considered to enable dual-mode operation with the optimum compression ratio for both LTC and conventional diesel combustion regimes.

Beyond conventional and low-temperature diesel combustion strategies, LIVC strategies were also explored as an option for controlling homogeneous charge compression ignition (HCCI) combustion [27,28,29]. However, the use of negative valve overlap (NVO) and exhaust rebreathing strategies became more prevalent for HCCI control.

Beyond the early RCCI studies using a LIVC strategy [5,13,14], limited exploration of dual-fuel operation with varied effective compression ratio has been conducted. Building off prior work on a gasoline-diesel dual-fuel strategy employed on a multi-cylinder, heavy-duty diesel engine [8,9], this study explores the performance and emissions impact of varying the effective compression ratio through the use of EIVC and LIVC strategies.

EXPERIMENTAL DETAILS

EQUIPMENT

The test engine used in this study is a MY2010 Navistar MaxxForce 13 six-cylinder heavy-duty diesel engine, an evolution of the engine used in previous research by [8,9]. A schematic of the test engine configuration is shown in Figure 1, along with basic engine specifications in Table 1. The base engine features an air system configured for high EGR delivery, utilizing two-stage turbocharging (with interstage cooling) and a dual-pass EGR cooler with high and low temperature stages. The stock 2200 bar capable common-rail diesel fuel injection system is maintained.

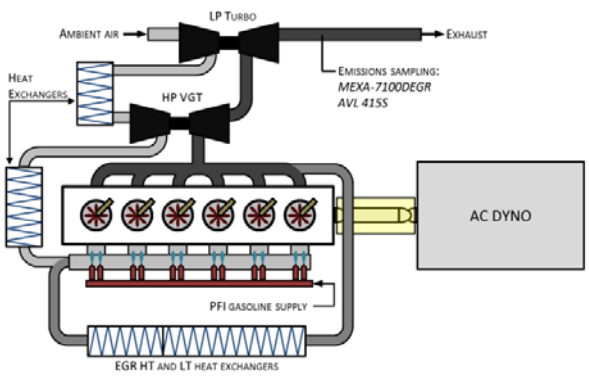

Figure 1. Schematic of test engine configuration.

Table 1. Engine Specifications.

	Navistar 13L DF
Cylinders [-]	6
Bore [mm]	126
Stroke [mm]	166
Displacement [L]	12.4
Base Geometric CR[-]	17:1
$P_{INJ,diesel,max}$ [bar]	2200
$P_{INJ,gasoline}$ [bar]	6

Several alterations to the production engine were made to enable and enhance low-temperature dual-fuel combustion. A rematched set of turbochargers, including a variable geometry (VGT) high-pressure turbocharger, are implemented to increase the EGR driving capacity. EGR is used to reduce combustion temperatures for lower NO_x emissions levels, to mitigate high peak pressure rise rates, and to increase the ignition delay after diesel injection. A modified intake manifold is used which incorporates two port fuel injection (PFI) gasoline injectors per cylinder. The gasoline fuel is injected at 6 bar above intake manifold pressure directed at the intake runner of each cylinder. Gasoline is supplied by an externally mounted, electrically-driven pump; energy consumed for gasoline fuel delivery is negligible and therefore not included in brake thermal efficiency calculations.

Additionally, the engine employs a production-intent prototype variable valve actuation (VVA) system developed by Jacobs Vehicle Systems (JVS) [30]. The VVA system utilizes a hydraulic lost-motion mechanism to provide the ability to control the length of intake valve events by varying the opening (not used in the current work) and closing time of the intake valves. Varied intake valve lift is not utilized within this work. By closing the intake valve earlier or later than conventional timing, the effective compression ratio – and therefore the ratio between compression and expansion ratio – can be reduced. The engine's geometric compression ratio – 17:1, an increase over the 14:1 geometric compression ratio employed in earlier work [8,9] – remains constant. Additionally, the expansion ratio remains constant, at a value close to the geometric compression ratio, due to fixed exhaust cam timing.

The variable valve actuation system, as designed, provides for intake valve close ranging from the earliest timing of 280°BTDC (440°ATDC) to the latest timing of 80°BTDC (640°ATDC), as illustrated in Figure 2. This provides a geometric compression ratio range from 9:1 to 17:1 using both early and late intake valve closing strategies. The IVC timing specified in this paper is nominal, though benchmarking with valve proximity sensors shows it matches valve timing at 1.5 mm lift. Valve timing is adjustable on an individual cylinder basis, with cycle-to-cycle control response.

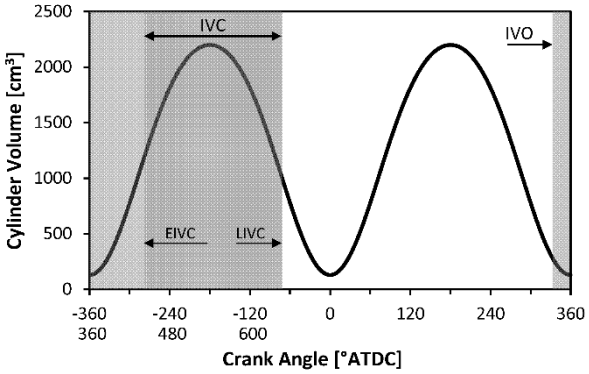

Figure 2. Range of intake valve close (dark shading) with VVA system, shown with respect to overall intake valve event (light shading) and cylinder volume (line).

Stock EGR and interstage intake air cooling systems are maintained. A building process water system is used for cooling heat exchangers in the high and low temperature engine coolant loops, and to directly cool the high pressure charge air cooler. Cooling systems were tuned using Navistar internal metrics to mimic heat rejection available in a production vehicle. Intake and exhaust restrictions were likewise adjusted to simulate vehicle air filtration systems along with exhaust aftertreatment and muffler restrictions. Constant restrictions were used across all tested conditions.

Fuel flow, both gasoline and diesel, is measured with Coriolis-type flowmeters. Low speed measurements of engine operating parameters, including temperatures, pressures, emissions, and fuel flow are logged at 10 Hz. Crank-angle resolved measurements of cylinder pressure are collected using Kistler 6125B transducers in all six cylinders at 0.1 crank angle degree resolution for 500 engine cycles. A 3 kHz low-pass filter is used to suppress significant cylinder pressure oscillation due to chamber resonance.

Start of injection timing, both as a reported value and used in computation of ignition delay, is determined from ECU command and not directly measured from injector current.

Gaseous emissions are measured using a standard 5-gas analyzer (Horiba MEXA-7100DEGR), which includes CO_2 measurements in the intake for EGR calculation. An AVL 415 Smoke Meter is used for soot emissions measurements.

TEST FUELS

The dual-fuel operating strategy employed in this study uses two fuels concurrently: a low-reactivity fuel (gasoline) along with a high-reactivity fuel (diesel). The gasoline used in this study was EEE certification gasoline, while the diesel was an ultra-low sulfur (ULSD) certification diesel fuel with typical diesel fuel properties and a cetane number of 44. Relevant properties of the two fuels are listed in Table 2.

Table 2. Test Fuel Properties.

	GASOLINE	DIESEL
Density [kg/L]	0.743	0.851
Net HV [MJ/kg]	42.5	42.8
RON [-]	97	-
MON [-]	89	-
CN [-]	-	44
Aromatics [%]	32	28
Olefins [%]	1	1
Saturates [%]	68	71
C:H Ratio	1.87	1.88
Sulfur [ppm]	28	10
T10 [°C]	50	214
T50 [°C]	104	259
T90 [°C]	158	317

EFFECTIVE COMPRESSION RATIO CALCULATION

A pressure based method [26,31] for computing effective compression ratio (ECR) is utilized within this work to reflect the impact of early or late intake valve closing strategies. Geometry-based effective compression ratio, which compares cylinder volume at specified IVC to the minimum clearance volume, is not fully representative of the compression process. Aspects not accounted for in a volume-based measurement include the compression effect of charge momentum and of piston motion [26]. These effects are clearly observed with late intake valve close where charge compression is observed as the piston expels charge back through a nearly-closed intake valve. The pressure based method used in this work, portrayed in Figure 3, uses cylinder pressure measurements to extract an effective IVC volume for effective compression ratio calculation. The polytropic compression curve, fit to the experimental cylinder pressure data, is extrapolated down to intersect the intake manifold pressure. The cylinder volume at this intersection point is used as the effective IVC volume for ECR calculation.

Within this work, effective CR is calculated on a 500-cycle averaged pressure trace for each cylinder, and the overall engine-average effective CR value reported. The standard deviation of effective compression ratio across all cylinders, not accounting for any uncertainty in the base measurements, is typically around ±0.25 with a maximum variation less than ±0.5.

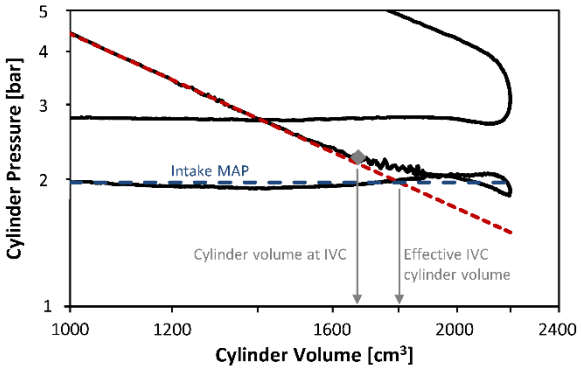

Figure 3. Cylinder pressure as a function of cylinder volume, diagraming the method used for computation of pressure-based effective compression ratio. Cylinder volume at point where extrapolated polytropic compression line intersects intake manifold pressure is used as maximum cylinder volume for ECR calculation.

Figure 4 reports the resulting effective compression ratios for the tested IVC conditions within this work, along with a line showing the computed effective compression ratio based on cylinder volume for a given IVC condition. The range of tested IVC settings include both early close, from 240-225°BTDC (effective CR of 12.8-14.8), and late close, from 130-110°BTDC (effective CR of 13.9-15.3). The deviation between effective CR computed from cylinder pressure characteristics to that based on cylinder volume is apparent in Figure 4 and Figure 5. Within the range of IVC conditions tested in this work, the late intake valve close conditions shift towards higher ECR levels than the early intake valve close conditions – the opposite of the trend observed in volume-based ECR.

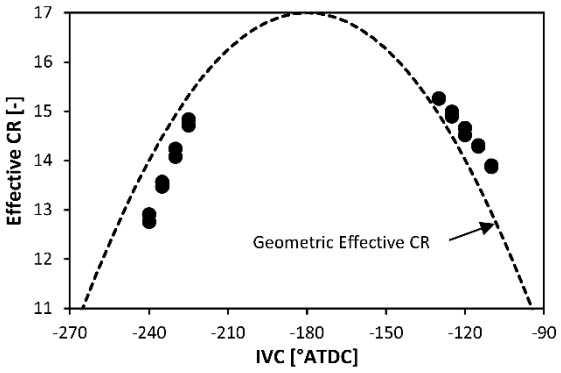

Figure 4. Effective compression ratio as a function of intake valve close (IVC) timing. Geometric effective compression ratio (line) plotted in addition to pressure-based effective compression ratio (data points).

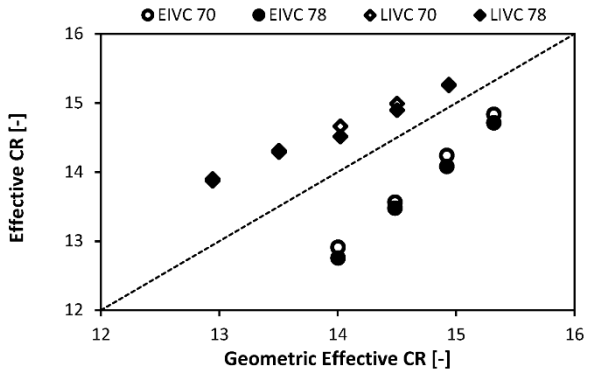

Figure 5. Effective compression ratio as a function of geometric compression ratio for EIVC and LIVC strategies.

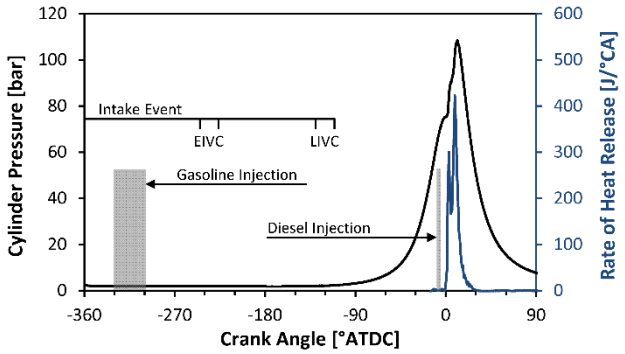

Figure 6. Representative dual-fuel combustion strategy with PFI injection of gasoline during intake stroke and start of combustion coupled to the direct diesel injection.

OPERATING CONDITIONS

Testing was conducted at 1200 rpm with an engine load of 8.2 bar BMEP, a light-mid load (35%) operating condition for the test engine configuration. Combustion phasing (location of 50% mass fraction burned) is fixed at 9±0.5°ATDC using cylinder pressure feedback control over the individual cylinder diesel injection timing. This combustion phasing was maintained across all engine cylinders. With engine performance characteristics strongly tied to combustion phasing, constant combustion phasing was used to mitigate any secondary effects.

Cylinder pressure is limited to 220 bar while maximum rate of pressure rise (for each cylinder, measured on an unfiltered cylinder pressure signal) is limited to less than 15 bar/degree. This limit is established as an outer boundary based on engine hardware durability – NVH concerns (combustion noise) is not the critical factor. NO_x emissions are limited to less than 0.27 g/kW-hr (0.20 g/hp-hr) based on EPA 2010 emissions standards for heavy-duty onroad engines. Soot emissions are not explicitly limited; they are measured and reported. Likewise, explicit limits are not placed on CO or HC emissions, though they are evaluated. Stable operation was maintained at each operating point, with a COV of engine-averaged IMEP less than 2% for all tested conditions.

DUAL-FUEL STRATEGY

The dual-fuel combustion mode splits the fuel introduction between two fuels of differing reactivity: a low-reactivity gasoline fuel (introduced via port injection during the intake stroke) and a high-reactivity diesel fuel (introduced via direct injection into the cylinder during the compression stroke). Within this work, two different fuel splits are examine, with 70% and 78% of the fuel energy delivered by the port-injected gasoline fuel. A schematic of typical gasoline and diesel injection timings as related to a pressure trace is included in Figure 6.

The single gasoline port fuel injection occurs during the intake stroke, with a constant start of injection at 330°BTDC for all test cases. Gasoline injection duration covers the range of 3.9-4.2 ms (28-30°CA). Varying the start of the gasoline injection, across a range of 300-400°BTDC, did not measurably alter combustion or emissions behavior at steady-state conditions.

A single diesel injection strategy is used, with the injection phased close in proximity to top dead center (0-15°BTDC). This differs in strategy from notable previous works [5,6] and is comparable to the “CM1” mode used in [8,9]. The timing of the diesel injection is used to control combustion phasing: combustion operates in a regime where diesel SOI and combustion phasing are closely coupled. Maintaining this direct relationship offers enhanced combustion control. The use of this strategy was selected based on earlier results showing that early phased diesel injections, whether single or multiple injections, are limited to lower load ranges than the single-injection strategy due to early autoignition [8,32].

Cooled exhaust gas recirculation (EGR) was used for all tested operating conditions. Air dilute combustion strategies, though successfully employed in previous research at low-load conditions [5,16] were not considered here. EGR quantity varies in the range of 40-45% - to minimize efficiency losses from pumping work, the EGR valve was maintained in a full-open position, with EGR level controlled using VGT vane position to maintain combustion within the desired NO_x emissions and peak pressure rise rate levels.

RESULTS AND ANALYSIS

OPERATION AND COMBUSTION CHARACTERISTICS

The use of EIVC or LIVC valve strategies has two principal effects on engine operation: (1) reducing the effective compression ratio and (2) reducing the trapped mass and, therefore, the massflow through the engine system. As noted previously, control parameters are varied across the range of tested IVC conditions to maintain dual-fuel operation at a nominal fixed combustion phasing within the NO_x emissions

and peak pressure rise rate constraints. Accordingly, these variations will impact the resulting engine behavior, and are a key factor in explaining the observed trends

Reduced trapped charge mass accompanies the lower effective compression ratio delivered by early or late intake valve close timings. EIVC reduces the charge mass due to a shorter intake duration, eliminating the later portion of the intake stroke and subsequent inducted charge volume. With LIVC, a portion of the charge mass inducted during the (full) intake stroke is expelled out the open intake valves during the initial portion of the compression stroke. An increase in boost pressure, to increase charge density, is required to compensate for the reduced trapped charge volume. In this work, no significant changes to the air system hardware were performed to maintain constant trapped mass. As shown in Figure 7, trapped mass decreases with decreasing effective compression ratio for both EIVC and LIVC strategies.

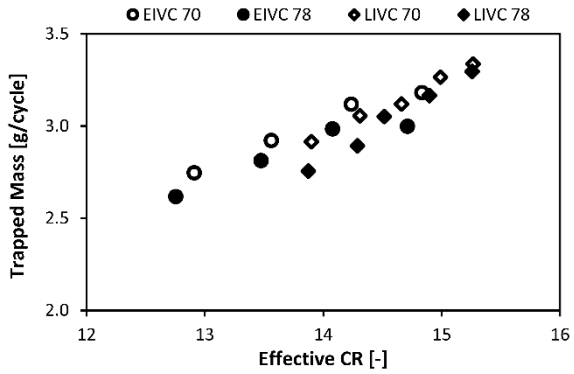

Figure 7: Trapped charge mass as a function of effective compression ratio.

For both fueling fractions, 70% and 78% gasoline, the trapped mass for the EIVC conditions are higher than for the LIVC conditions at the same effective compression ratio. This is expected based on the pressure-based method of computing effective compression ratio. As shown in Figure 5, there is a divergence in ratio between pressure-based effective compression ratio and geometric compression ratio. For a given pressure-based effective compression ratio, the corresponding geometric compression ratio for the EIVC conditions will be greater than the LIVC conditions. Accordingly, the trapped charge volume (and therefore trapped charge mass) for EIVC conditions will therefore be greater than the corresponding LIVC condition. The divergence of the pressure and geometric effective compression ratios increases as the compression ratio decreases – the difference in trapped mass trends accordingly.

Minor offsets in trapped mass are observed between the 70 and 78% gasoline fueling conditions, although consistent trends are observed. As discussed throughout the results and analysis, the higher fueling fraction is more susceptible to high rates of pressure rise – to compensate, higher EGR levels are used. Although the EGR is cooled in a two-stage cooler, the resulting intake manifold temperature increases with the higher EGR levels. In addition, increased EGR reduces flow through the turbochargers, decreasing boost levels. The combination of reduced boost level and higher intake temperature yields lower charge density, and a subsequent reduction in trapped mass.

Behavior of lambda, the relative air/fuel ratio, with respect to effective compression ratio mirrors the observed trends in trapped mass, as shown in Figure 8. Lambda decreases with decreasing effective compression ratio for both EIVC and LIVC strategies at both fueling ratios.

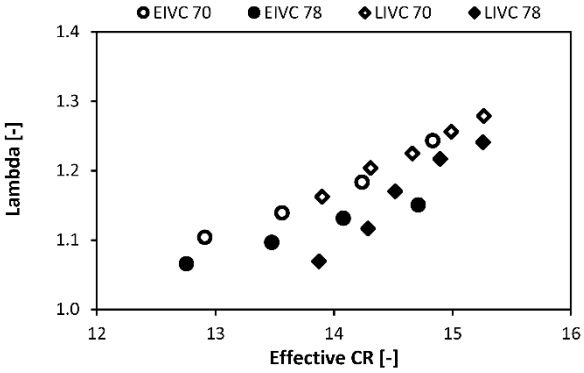

Figure 8: Lambda as a function of effective compression ratio.

The reduction in trapped mass is principally a reduction in trapped air and EGR mass, not a reduction in fueling rate. Barring a major change in overall brake thermal efficiency (not observed, as discussed in greater detail later), fuel mass will remain in a narrow window for all of the operation conditions since engine load remains constant. Note that at the lowest effective compression ratios, lambda is approaching stoichiometric conditions.

As acknowledged, EGR varies across the operating conditions; it is used as the principal control for managing NO_x and peak pressure rise rate (PPRR) levels to maintain operation within the specified targets. Figure 9 shows both EGR, calculated as a volumetric ratio using intake and exhaust CO_2 measurements, and calculated intake oxygen concentration.

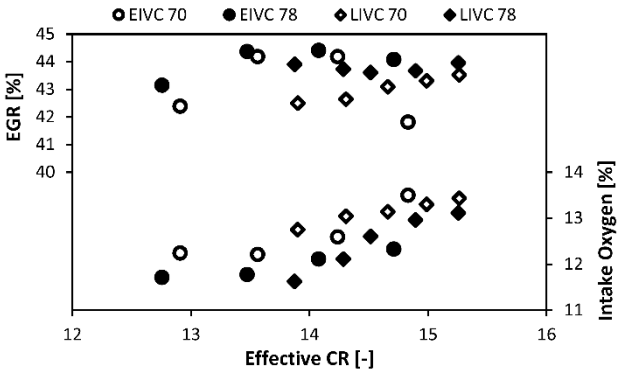

Figure 9: Volumetric EGR fraction and intake oxygen concentration across the range of effective compression ratios.

For the LIVC conditions, EGR fraction decreases slightly with decreasing effective compression ratio, while for the conditions using EIVC, the EGR fractions decreases at low and high effective compression ratios.

Overall intake oxygen content consistently decreases with lower effective compression ratio for all operating conditions, including both EIVC and LIVC strategies and both fueling fractions. Intake oxygen content for the 70% gasoline conditions is greater (and EGR lower) than for the comparable 78% gasoline conditions, reflecting the need to suppress greater combustion NO_x and PPRR levels with the higher gasoline fraction.

The change in effective compression ratio, brought about by varying IVC, reduces the compression pressure, with a corresponding impact on combustion. Shown in Figure 10 are traces of cylinder pressure and rate of heat release (RoHR) for dual-fuel operation with a range of early IVC conditions at a set operating point with fixed engine load and comparable air system settings. As effective compression ratio decreases, from 14.1:1 to 12.8:1, over the range of conditions shown, decreased cylinder pressure is observed during both the compression and combustion-expansion portions of the trace.

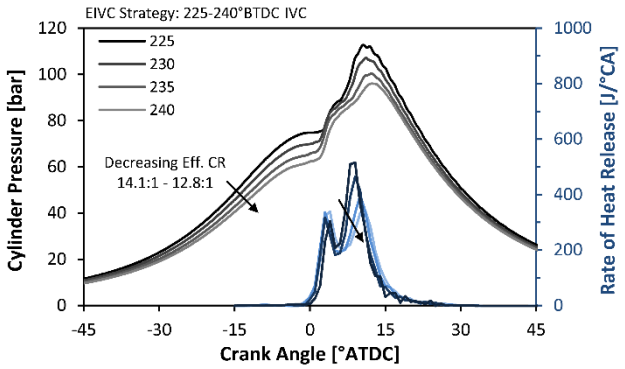

Figure 10: Cylinder pressure and rate of heat release (RoHR) traces across a range of EIVC conditions at 1200 rpm, 8.2 bar BMEP, with 78% gasoline/diesel fuel fraction, and fixed combustion phasing.

Also apparent is a reduction in peak heat release rate as compression ratio decreases, reflecting a reduction in the second phase of the combustion heat release. One combustion characteristic of the tested dual-fuel strategy is a two-stage heat release, with the first stage (initial spike in RoHR) reflecting combustion of the diesel fuel and entrained gasoline while the second (second spike in RoHR) is the combustion of the remaining premixed (gasoline) charge [8,9]. There is similar magnitude in the first spike of heat release rate, reflecting the similar character of the diesel injections across the range of conditions. The characteristics of the initial dual-fuel heat release are largely driven by the diesel injection process, which is comparable for all points. Diesel injection pressure remains constant (1850 bar), and the overall diesel injection quantity varies less than 1% across the range of IVC conditions shown in Figure 10. The second heat-release peak decreases with lower effective compression ratio, and increases in duration. The lower pressure conditions in-cylinder yield slower kinetic reaction rates, and a slower heat release.

Figure 11 illustrates combustion progression for the tested conditions, including SOI, 10% and 50% mass fraction burned (MFB) points, and the ignition delay specified as SOI-10% MFB duration. Engine testing used a cylinder pressure feedback control to maintain a nominally-constant 50% MFB location at approximately 8.5±0.5°ATDC. There is a slight retard in CA50 as effective compression ratio decreases, owing to differences in the heat release calculation used by the real-time feedback control and the analysis methods. Ignition delay consistently increases as effective compression ratio decreases for all tested conditions, requiring earlier SOI to maintain constant phasing. For a given effective compression ratio, ignition delay remains comparable between conditions using EIVC and those using LIVC. The lower oxygen levels and reduced pressure of the 78% gasoline fueling cases generally yield slightly longer ignition delay than the 70% gasoline conditions.

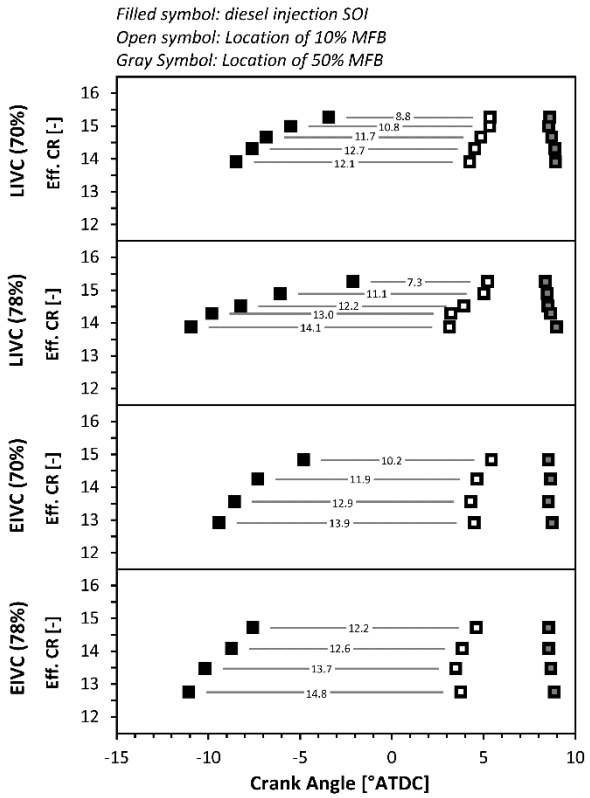

Figure 11: Combustion progression, including SOI, location of 10% and 50% mass fraction burned, and ignition delay as a function of effective compression ratio for each fuel and valve strategy.

EMISSION CHARACTERISTICS

Figure 12 reports the NO_x and soot emissions over the range of effective compression ratios tested. As noted before, prescribed limits on NO_x emissions (0.27 g/kW-hr) based on EPA 2010 emissions standards [2] are maintained for all conditions. NO_x emissions therefore remain at the specified maximum target level for most conditions. The exception are conditions where greater EGR levels are required for suppression of peak pressure rise rate than for NO_x emissions; NO_x emissions are then lower than the specified maximum limit.

To maintain the 0.27 g/kW-hr NO_x emissions level, particulate emissions are correspondingly high, though not explicitly limited in this study. As shown in

Figure 12, the soot emissions remain relatively constant for most conditions, increasing only at the highest effective compression ratios. For these high effective compression ratio conditions (LIVC strategy), the ignition delays, as reported in Figure 11, are the lowest of all the test conditions. Soot emissions generally increase with shorter ignition delay and, for conditions with an ignition delay (SOI-10%MFB) of 10°CA or less, the increase in soot emissions is directly proportional to the reduction in ignition delay. For a given ignition delay, the 70% gasoline fraction conditions have higher soot emissions. These indicate that, as expected, the soot emissions primarily result from the direct diesel injection and not the premixed gasoline mixture.

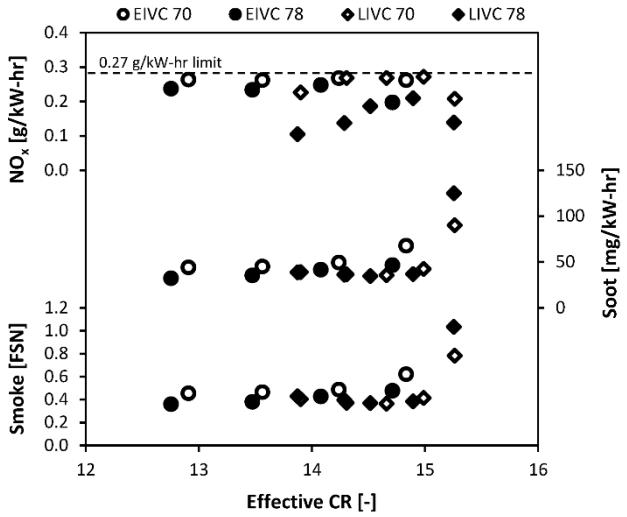

Figure 12: NO_x and soot emissions as a function of effective compression ratio.

Trends in CO and unburned HC emissions are shown as a function of effective compression ratio in Figure 13. In low-temperature dual-fuel combustion modes, CO emissions are largely driven by incomplete combustion of premixed fuel in the squish region [33]. With respect to effective compression ratio, CO emissions generally decrease at lower effective compression ratios – higher combustion temperatures, due to the decreased overall charge mass, yield more complete fuel oxidation. Balancing this, the same effects in intake oxygen content and trapped mass which yield lower NO_x emissions at certain conditions also increase incomplete oxidation in the squish regions, yielding higher CO emissions. Additionally, CO emissions are greater for the lower (70%) gasoline fueling rate. This suggests the increased CO results from the higher diesel quantity, though another probable explanation is that the corresponding decrease in premixed (gasoline) fraction increases the overleaning of the premixed charge in regions away from the diesel plumes, increasing incomplete combustion and CO emissions.

Unburned HC emissions remain constant across the range of effective compression ratios for both fueling rates and valve strategies, in the range of 1-2 g/kW-hr. This is consistent with results reported previously [8,9]. For the type of piston geometry (stepped, reentrant toroidal bowl) used here, HC emissions are primarily from crevice and squish regions.

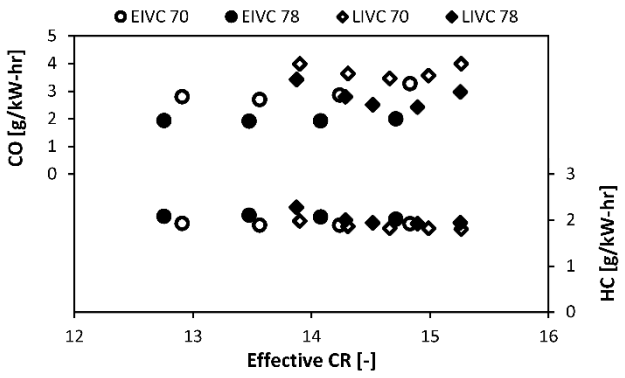

Figure 13: CO and HC emissions as a function of effective compression ratio.

PRESSURE RISE RATE AND COMBUSTION NOISE

Figure 14 displays both peak pressure rise rate (PPRR) and combustion noise as a function of effective compression ratio for the tested conditions. Both peak pressure rise rate and combustion noise are computed on raw (unfiltered) individual cycle pressure traces from each cylinder, then averaged across all 500 cycles, and subsequently across all cylinders. Plotted points represent this overall engine average value, with the error bars showing the highest and lowest individual cylinder levels.

As noted in the Experimental Details section, peak pressure rise rate was limited to less than 15 bar/degree for all cylinders. With cylinder-to-cylinder variations present in the engine, the average PPRR level can be significantly less than the 15 bar/degree limit while an individual cylinder is at the limit. As visible in Figure 14, substantial cylinder-to-cylinder variation exists in peak pressure rise rate and combustion noise. EGR misdistribution can be a significant factor at higher EGR levels such as the 40-45% used in these tests, as shown in Figure 9.

Combustion noise is calculated using the AVL combustion noise metric (A+CAV filters applied). While operation limits for hardware preservation were initially established in relation to peak pressure rise rate, computed combustion noise results are also included since recent work indicates PPRR does not necessarily directly correlate with measured combustion noise [33]. For all tested conditions, average combustion noise remains within a range of 89-93 dB. Trends in combustion noise largely mirror those observed in peak pressure rise rate. In Figure 14, error bars on noise data represents one standard deviation of computed noise measurements across all cylinders and 500 cycles.

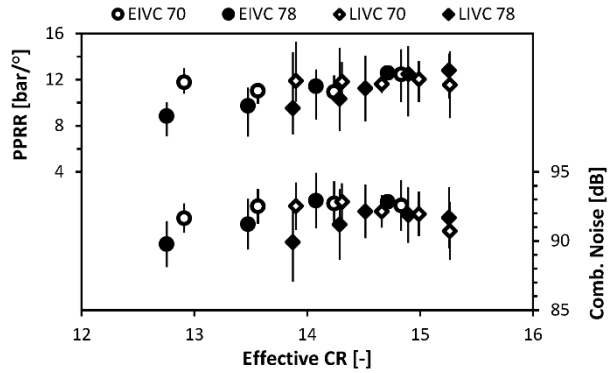

Figure 14: Peak pressure rise rate and combustion noise as a function of effective compression ratio. Points represent overall engine averages, while error bars show range of individual cylinder values for PPRR and one standard deviation for engine noise.

EFFICIENCY TRENDS

Brake thermal efficiency (BTE), along with both gross and net indicated thermal efficiency (ITE_{GROSS} and ITE_{NET}, respectively) are compared between EIVC and LIVC strategies in Figure 15. Gross indicated efficiency is the conversion of fuel energy to indicated work output from only the combustion cycle, while net indicated efficiency is conversion of fuel energy to total indicated work including both combustion and gas exchange cycles.

Uncertainty in the computed efficiency was quantified – error bars are omitted from Figure 15 for clarity. Uncertainty for the reported efficiencies combine measurement uncertainty (measurement fluctuation as characterized by one standard deviation of measured values) and instrument uncertainty. Assessed uncertainty is as follows: ±1% for brake thermal efficiency (BTE), and ±0.5% for gross and net indicated thermal efficiency.

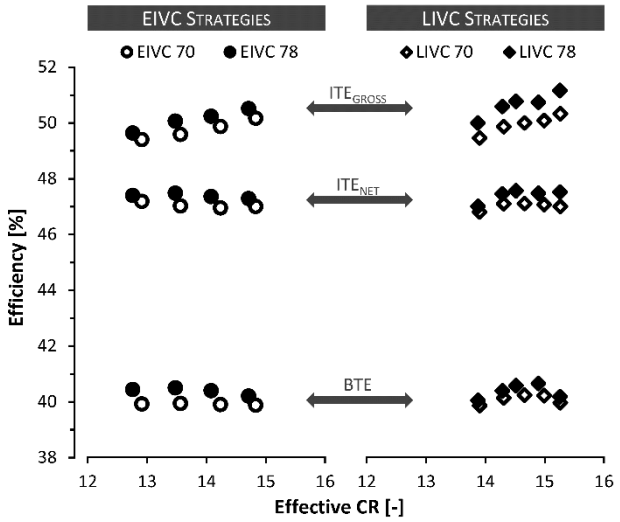

Figure 15: Comparison of efficiencies, including gross and net indicated thermal efficiency (ITE_{GROSS} and ITE_{NET}) and brake thermal efficiency (BTE) between EIVC and LIVC strategies as a function of effective compression ratio.

Peak brake thermal efficiency is within 0.1-0.3% between the early and late intake valve closing strategies for a given gasoline fueling fraction, within the overall uncertainty level. The highest measured BTEs for the 78% gasoline case are 40.5% (EIVC) and 40.6% (LIVC) at effective compression ratios of 13.5:1 (235°BTDC IVC) and 14.9:1 (125°BTDC IVC), respectively. General trends in brake thermal efficiency are similar between EIVC and LIVC strategies: an optimum effective CR with decreasing BTE observed as effective CR moves away (to both higher and lower effective CR) from the optimum point. For the EIVC conditions, however, the rate of efficiency decrease is much flatter than for the LIVC cases.

The 78% gasoline fueling fraction conditions delivered higher BTE results than the comparable 70% gasoline cases – the efficiency increase manifests in higher ITE_{GROSS} and, with comparable pumping and friction losses, is consistent through both ITE_{NET} and BTE.

Consistent trends in both gross and net indicated thermal efficiency are observed, with ITE_{NET} remaining relatively constant with respect to effective compression ratio, and ITE_{GROSS} decreasing with lower effective compression ratio.

To further understand the trends in efficiency observed as a function of IVC timing, a breakdown of process efficiencies was conducted. Reflecting the methodology employed in [35], engine energy flow is represented by four key efficiencies: combustion (incomplete combustion losses), thermodynamic (thermal losses), gas exchange (pumping losses), and mechanical (friction losses). Multiplication of all four efficiencies yields the brake thermal efficiency.

Combustion efficiency is computed from the exhaust gas emissions using the method prescribed in [36], adapted for dual-fuel combustion and using updated HC molecular weights per [37]. Thermodynamic efficiency is the fraction of gross indicated power (IMEP from the combustion cycle only) to the released fuel energy (as defined by fuel flow, heating value, and combustion efficiency). Gas exchange efficiency is computed by dividing net indicated power (IMEP from full cycle, including pumping loop) with gross indicated power (IMEP from the combustion cycle only). Mechanical efficiency is the fraction of brake power to net indicated power. These four intermediate efficiencies are shown in Figure 16, reporting combustion and mechanical efficiency, and Figure 17, showing thermodynamic and gas exchange efficiencies.

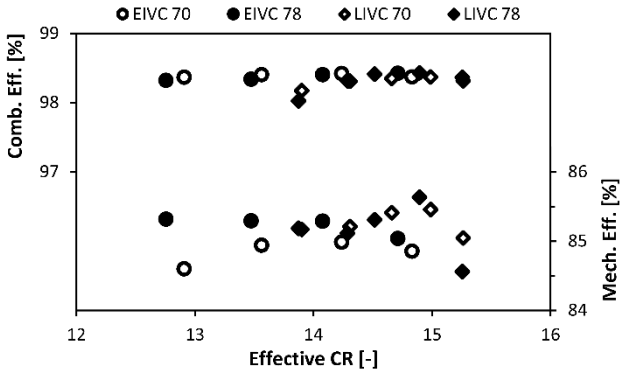

Figure 16: Combustion and mechanical efficiency as a function of effective compression ratio.

As shown in Figure 16, combustion efficiency remains relatively constant across the range of tested effective compression ratios, with levels in the range of 98-98.5%. No significant differences in combustion efficiency are observed, and overall levels are comparable to the results reported in [8,9]. Additionally, mechanical efficiency (friction losses) remains within a 1% range across the span of tested effective compression ratios. Minor variations, but no consistent trends, are apparent between different valve strategies and fueling rates.

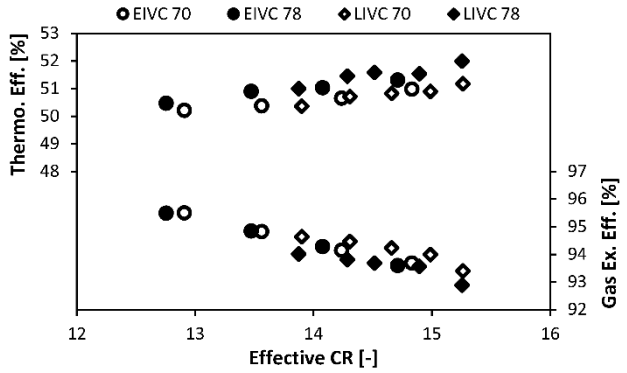

Figure 17: Thermodynamic and gas exchange efficiency as a function of effective compression ratio.

Gas exchange efficiency, as shown in Figure 17, increases linearly with reduced effective compression ratio for both EIVC and LIVC strategies. The reduced engine massflow at lower effective compression ratios, tracking the changes in trapped mass reported in Figure 7, yields reduced pumping losses.

However, while the gas exchange efficiency improves as effective compression ratio decreases, the thermodynamic efficiency drops across the same range at a comparatively similar magnitude. Lower thermodynamic efficiency is a reflection of increased thermal losses at lower effective compression ratios. The net result is that the benefits in improved pumping efficiency are largely offset by the increased losses in thermodynamic efficiency. This is also apparent in Figure 15 which shows largely flat trends in ITE_{NET} as a function of effective compression ratio.

Additional thermodynamic losses are likely related to increasing in-cylinder heat loss. Exhaust thermal losses decrease slightly as effective compression ratio decreases, while combustion phasing losses are mitigated by maintaining matched combustion timing and similar heat release characteristics. As the effective compression ratio decreases, comparable energy addition with reduced trapped charge mass yields higher cycle temperatures which drive increased thermal losses in-cylinder. While neither combustion heat losses nor combustion temperature are directly measured in this application, higher combustion temperatures can be inferred from exhaust temperature trends, given the common expansion ratio utilized in all cases. Exhaust gas temperatures, as shown in Figure 18, increase linearly with lower effective compression ratio, from 400-475°C across the range of tested conditions. Higher in-cylinder temperatures drive increased thermal losses in-cylinder, reducing thermodynamic efficiency.

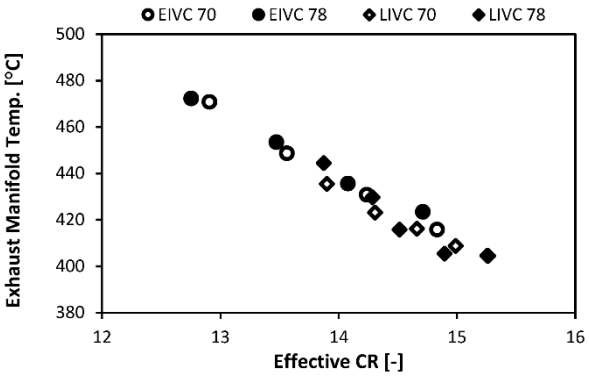

Figure 18: Exhaust manifold temperature as a function of effective compression ratio.

Note that higher in-cylinder temperatures are not in conflict with the constant (or decreasing) NO_x trends reported in Figure 12 earlier. Thermal NO_x formation is a local phenomenon and not directly a function of bulk gas temperature. Further, while an increase in the combustion temperature is usually accompanied by an increase in NO_x emissions due to higher thermal NO_x formation, this can be offset by a reduction in air/fuel ratio reflecting the lower intake oxygen content and reduced trapped mass.

CONCLUSIONS

A range of different intake valve closing timings, covering both early (EIVC) and late (LIVC) intake valve closing, were evaluated on a heavy-duty compression-ignition engine equipped with a variable valvetrain and operating using a gasoline-diesel dual-fuel strategy. Testing centered on a light-load operating condition using two different gasoline fueling fractions. From the results of these tests, the following conclusions are drawn:

Without changes to the engine air system accompanying the use of LIVC and EIVC strategies, combustion effects are strongly influenced by both the reduction in effective compression ratio and the changes in trapped mass. The pressure-based effective compression ratio calculation represents the changes in pressure conditions well, but does not fully account for effects from the changes in trapped mass.

Reduced massflow through the engine resulting from the EIVC and LIVC strategies reduces pumping work, increasing the gas exchange efficiency. However, the reduction in trapped mass yields higher combustion temperatures, increasing thermal losses, which decreases the thermodynamic efficiency, offsetting the reduction in pumping work. Accordingly, net indicated thermal efficiency remains relatively constant across the range of IVC conditions. With IVC timing having minimal impact on engine friction, brake thermal efficiency also remains relatively constant across the range of conditions tested.

ACKNOWLEDGMENTS

This study was supported by the U.S. Department of Energy (DOE), the National Energy Technology (NETL) office, under cooperative agreement “SuperTruck – Development and Demonstration of a Fuel-Efficient Class 8 Tractor & Trailer” DOE Contract: DE-EE0003303. The authors wish to thank Roland Gravel, Gurpreet Singh, and Ken Howden of DOE and Ralph Nine of NETL for their continuing support.

Crank-angle resolved data processing, including calculation of heat release, was performed using AVL Concerto. The authors wish to express their gratitude to staff at AVL North America Inc. for their support.

REFERENCES

1. “Greenhouse Gas Emissions Standards and Fuel Efficiency Standards for Medium- and Heavy-Duty Engines and Vehicles,” *Federal Register* 76(179): 57106-57513, 2011.
2. “Control of Air Pollution from New Motor Vehicles: Heavy-Duty Engine and Vehicle Standards and Highway Diesel Fuel Sulfur Control Requirements,” *Federal Register* 66(12): 5002-5193, 2001.
3. "Recovery Act—Systems Level Technology Development, Integration, and Demonstration for Efficient Class 8 Trucks (SuperTruck) and Advanced Technology Powertrains for Light Duty Vehicles (ATP-LD)," DE-FOA-0000079, Department of Energy: Washington, D.C., 2009.
4. De Ojeda, W. and Rajkumar, M., "Engine Technologies for Clean and High Efficiency Heavy Duty Engines," *SAE Int. J. Engines* 5(4):1759-1767, 2012, doi:10.4271/2012-01-1976.
5. Kokjohn, S., Hanson, R., Splitter, D., and Reitz, R., "Experiments and Modeling of Dual-fuel HCCI and PCCI Combustion Using In-Cylinder Fuel Blending," *SAE Int. J. Engines* 2(2):24-39, 2010, doi:10.4271/2009-01-2647.
6. Hanson, R., Kokjohn, S., Splitter, D., and Reitz, R., "An Experimental Investigation of Fuel Reactivity Controlled PCCI Combustion in a Heavy-Duty Engine," *SAE Int. J. Engines* 3(1):700-716, 2010, doi:10.4271/2010-01-0864.
7. Joo, S., Alger, T., Chadwell, C., De Ojeda, W. et al., "A High Efficiency, Dilute Gasoline Engine for the Heavy-Duty Market," *SAE Int. J. Engines* 5(4):1768-1789, 2012, doi:10.4271/2012-01-1979.
8. Zhang, Y., Sagalovich, I., De Ojeda, W., Ickes, A. et al., "Development of Dual-Fuel Low Temperature Combustion Strategy in a Multi-Cylinder Heavy-Duty Compression Ignition Engine Using Conventional and Alternative Fuels," *SAE Int. J. Engines* 6(3):1481-1489, 2013, doi:10.4271/2013-01-2422.
9. Ickes, A., Wallner, T., Zhang, Y., and De Ojeda, W., "Impact of Cetane Number on Combustion of a Gasoline-Diesel Dual-Fuel Heavy-Duty Multi-Cylinder Engine," *SAE Int. J. Engines* 7(2):860-872, 2014, doi:10.4271/2014-01-1309.
10. Teetz, C., Bergmann, D., Schneemann, A., et al., "MTU HCCI Engine with Low Raw Emissions," *MTZ* 73(9):4-9, 2012.
11. De Ojeda, W., Zhang, Y., Xie, K., Han, X. et al., "Exhaust Hydrocarbon Speciation from a Single-Cylinder Compression Ignition Engine Operating with In-Cylinder Blending of Gasoline and Diesel Fuels," SAE Technical Paper 2012-01-0683, 2012, doi:10.4271/2012-01-0683.
12. Zhang, Y., De Ojeda, W., and Wickman, D., "Computational Study of Combustion Optimization in a Heavy-Duty Diesel Engine Using In-Cylinder Blending of Gasoline and Diesel Fuels," SAE Technical Paper 2012-01-1977, 2012, doi:10.4271/2012-01-1977.
13. Hanson, R., Splitter, D., and Reitz, R., "Operating a Heavy-Duty Direct-Injection Compression-Ignition Engine with Gasoline for Low Emissions," SAE Technical Paper 2009-01-1442, 2009, doi:10.4271/2009-01-1442.
14. Kokjohn, S., Hanson, R., Splitter, D., Reitz, R. “Fuel reactivity controlled compression ignition (RCCI): a pathway to controlled high-efficiency clean combustion,” *International Journal of Engine Research* 12(3): 209-226, 2011, doi:10.1177/1468087411401548.
15. Hanson, R., Kokjohn, S., Splitter, D., and Reitz, R., "Fuel Effects on Reactivity Controlled Compression Ignition (RCCI) Combustion at Low Load," *SAE Int. J. Engines* 4(1):394-411, 2011, doi:10.4271/2011-01-0361.
16. Splitter, D., Hanson, R., Kokjohn, S., and Reitz, R., "Reactivity Controlled Compression Ignition (RCCI) Heavy-Duty Engine Operation at Mid-and High-Loads with Conventional and Alternative Fuels," SAE Technical Paper 2011-01-0363, 2011, doi:10.4271/2011-01-0363.
17. Miller, R., “Supercharging and Internal Cooling Cycle for High Output” *Transactions of the American Society of Mechanical Engineers* 69:453–457, 1947.
18. Edwards, S., Frankle, G., Wirbeleit, F., and Raab, A., "The Potential of a Combined Miller Cycle and

Internal EGR Engine for Future Heavy Duty Truck Applications," SAE Technical Paper 980180, 1998, doi:10.4271/980180.
19. Millo, F., Mallamo, F., and Mego, G., "The Potential of Dual Stage Turbocharging and Miller Cycle for HD Diesel Engines," SAE Technical Paper 2005-01-0221, 2005, doi:10.4271/2005-01-0221.
20. Imperato, M., Antila, E., Sarjovaara, T., Kaario, O. et al., "NOx Reduction in a Medium-Speed Single-Cylinder Diesel Engine using Miller Cycle with Very Advanced Valve Timing," SAE Technical Paper 2009-24-0112, 2009, doi:10.4271/2009-24-0112.
21. Benajes, J., Molina, S., Martín, J., Novella, R., "Effect of advancing the closing angle of the intake valves on diffusion-controlled combustion in a HD diesel engine," *Applied Thermal Engineering* 29(10): 1947-1954, 2009, doi: 10.1016/j.applthermaleng.2008.09.014.
22. Nevin, R., Sun, Y., Gonzalez D., M., and Reitz, R., "PCCI Investigation Using Variable Intake Valve Closing in a Heavy Duty Diesel Engine," SAE Technical Paper 2007-01-0903, 2007, doi:10.4271/2007-01-0903.
23. De Ojeda, W., "Effect of Variable Valve Timing on Diesel Combustion Characteristics," SAE Technical Paper 2010-01-1124, 2010, doi:10.4271/2010-01-1124.
24. Murata, Y., Kusaka, J., Odaka, M., Daisho, Y. et al., "Achievement of Medium Engine Speed and Load Premixed Diesel Combustion with Variable Valve Timing," SAE Technical Paper 2006-01-0203, 2006, doi:10.4271/2006-01-0203.
25. Murata, Y., Kusaka, J., Daisho, Y., Kawano, D. et al., "Miller-PCCI Combustion in an HSDI Diesel Engine with VVT," *SAE Int. J. Engines* 1(1):444-456, 2009, doi:10.4271/2008-01-0644.
26. He, X., Durrett, R., and Sun, Z., "Late Intake Valve Closing as an Emissions Control Strategy at Tier 2 Bin 5 Engine-Out NOx Level," *SAE Int. J. Engines* 1(1):427-443, 2009, doi:10.4271/2008-01-0637.
27. Agrell, F., Ångström, H., Eriksson, B., Wikander, J. et al., "Integrated Simulation and Engine Test of Closed Loop HCCI Control by Aid of Variable Valve Timings," SAE Technical Paper 2003-01-0748, 2003, doi:10.4271/2003-01-0748.
28. Agrell, F., Ångström, H., Eriksson, B., Wikander, J. et al., "Transient Control of HCCI Through Combined Intake and Exhaust Valve Actuation," SAE Technical Paper 2003-01-3172, 2003, doi:10.4271/2003-01-3172.
29. Strandh, P., Bengtsson, J., Johansson, R., Tunestål, P. et al., "Variable Valve Actuation for Timing Control of a Homogeneous Charge Compression Ignition Engine," SAE Technical Paper 2005-01-0147, 2005, doi:10.4271/2005-01-0147.
30. Schwoerer, J., Kumar, K., Ruggiero, B., and Swanbon, B., "Lost-Motion VVA Systems for Enabling Next Generation Diesel Engine Efficiency and After-Treatment Optimization," SAE Technical Paper 2010-01-1189, 2010, doi:10.4271/2010-01-1189.
31. Klein, M. and Eriksson, L., "Methods for Cylinder Pressure Based Compression Ratio Estimation," SAE Technical Paper 2006-01-0185, 2006, doi:10.4271/2006-01-0185.
32. Zhang, Y., De Ojeda, W., Jadin, D., Ickes, A., Wallner, T., Wickman, D. "Development of Dual-Fuel Engine for Class 8 Applications" Proceedings of the 2012 Directions in Engine-Efficiency and Emissions Research (DEER) Conference. 2012.
33. Splitter, D., Wissink, M., Kokjohn, S., and Reitz, R., "Effect of Compression Ratio and Piston Geometry on RCCI Load Limits and Efficiency," SAE Technical Paper 2012-01-0383, 2012, doi:10.4271/2012-01-0383.
34. Shahlari, A., Hocking, C., Kurtz, E., and Ghandhi, J., "Comparison of Compression Ignition Engine Noise Metrics in Low-Temperature Combustion Regimes," *SAE Int. J. Engines* 6(1):541-552, 2013, doi:10.4271/2013-01-1659.
35. Johansson, B. "The Combustion, Thermodynamic, Gas Exchange and Mechanical Efficiencies of HCCI Engines," Presented at SAE 2006 Powertrain and Fluid Systems Conference and Exhibition. Toronto, Ontario, Canada. October 16-19, 2006.
36. Stivender, D., "Development of a Fuel-Based Mass Emission Measurement Procedure," SAE Technical Paper 710604, 1971, doi:10.4271/710604.
37. "Part 1065--Engine Testing Procedures," Code of Federal Regulations, 40 CFR 1065.

CONTACT

Andrew Ickes
Argonne National Laboratory
9700 S. Cass Ave.
Lemont, IL 60439, USA
+001-630-252-9920
aickes@anl.gov

DEFINITIONS, ACRONYMS, ABBREVIATIONS

ATDC: After Top Dead Center
BMEP: Brake Mean Effective Pressure
BSFC: Brake Specific Fuel Consumption
BTDC: Before Top Dead Center
BTE: Brake Thermal Efficiency
CA10: Location of 10% mass fraction burned
CA50: Location of 50% mass fraction burned
CN: Cetane Number
COV: Coefficient of Variation
CR: Compression Ratio
ECR: Effective Compression Ratio
EEE: EPA Tier II Certification Gasoline
EGR: Exhaust Gas Recirculation
EIVC: Early Intake Valve Close
HC: Hydrocarbon
HCCI: Homogeneous Charge Compression Ignition
IMEP: Indicated Mean Effective Pressure
ITE_{GROSS}: Gross Indicated Thermal Efficiency
ITE_{NET}: Net Indicated Thermal Efficiency
IVC: Intake Valve Close
LIVC: Late Intake Valve Close
LTC: Low Temperature Combustion

MFB: Mass Fraction Burned
MON: Motor Octane Number
NMHC: Non-Methane Hydrocarbons
NO_x: Nitric Oxides (NO+NO2)
NVO: Negative Valve Overlap
PCCI: Premixed Charge Compression Ignition
PCI: Premixed Compression Ignition
PFI: Port Fuel Injection
PPRR: Peak Pressure Rise Rate
RCCI: Reactivity Controlled Compression Ignition
RoHR: Rate of Heat Release
RON: Research Octane Number
SOI: Start of Injection
T10: Distillation temperature for 10% recovery
T50: Distillation temperature for 50% recovery
T90: Distillation temperature for 90% recovery
ULSD: Ultra Low Sulfur Diesel
VGT: Variable Geometry Turbocharger
VVA: Variable Valve Actuation